

# Measurement of $K$ -values in Diamondback Hoppers using pressure sensitive pads

Kerry Johanson<sup>a,\*</sup>, Ray Bucklin<sup>b</sup>

<sup>a</sup>Engineering Research Center for Particle Science and Technology, University of Florida, PO Box 116135, Gainesville, FL 326116135, USA

<sup>b</sup>Agricultural and Biological Engineering, University of Florida, Gainesville, FL, USA

Received 4 October 2003; received in revised form 21 January 2004; accepted 26 January 2004

## Abstract

Measurement of wall loads in hoppers has been difficult due to the expense of constructing multiple loads cell measurement units in a hopper. Recent advances in measurement techniques have allowed significant improvements in the measurement of multiple point normal stresses in hoppers. This paper presents measurements of wall stresses using pressure sensitive pads made by TekScan™. The wall stresses in a Diamondback Hopper™ were measured, indicating significant spatial stress variation. These hopper stresses were used to compute spatially varying  $K$ -values using a modified Janssen stress approach. The Janssen stress ratio approach with varying  $K$ -values that were a function of local hopper slope angle generated wall load curves that captured the general behavior of the observed wall loads.

© 2004 Elsevier B.V. All rights reserved.

*Keywords:*  $K$ -value; Stress; Wall loads

## 1. Introduction

To predict the solids stress in silos, Janssen [1] introduced the concept of a constant ratio of the average vertical stress to the stress normal to the wall. Later, this concept was applied to converging hoppers.  $K$ -values depend on the hopper slope angle and wall friction angle. The hopper geometry also affects these values. For example,  $K$ -values in converging hoppers are greater than one while  $K$ -values in diverging hoppers are less than one. In addition, conical  $K$ -values are smaller than  $K$ -values for wedged shaped hoppers. The Diamondback Hopper™ converges in one direction and diverges in the other. Consequently,  $K$ -value computation in this unusual hopper geometry is not straightforward. This paper provides experimental measurements of  $K$ -values in Diamondback Hoppers™.

## 2. $K$ -values

A powder consists of individual grains of solid material. Each grain contact exhibits a Coulombic friction behavior.

When combined, these grain friction values result in a bulk property called internal friction. This property causes behaviors that distinguish a powder material from a fluid. Because of internal friction, powders form piles. Additionally, the ability of powders to generate stable structures (piles) allows bulk solid materials to develop differences in the stress magnitude on confining walls depending on the direction of the wall. For example, a static fluid placed in a container would cause the same normal stress on all wall surfaces at the same fluid depth. However, placing a bulk solid material in the same container will result in stresses at the same depth that depend on the local geometry and how the container was filled. The ratio of stresses normal to confining walls to vertical stresses in the bulk material is defined as the  $K$ -value, and has been used to explain observed loads on retaining walls. Wall stresses can exceed vertical stresses when the geometry of the confining boundary causes strains that compact material. Conversely, these wall stresses can be much lower than the vertical stresses if the boundary causes strains that allow material expansion. Soil mechanics practitioners take advantage of this property of granular materials when building retaining walls. Retaining walls pull away from material, activating a plastic stress state, allowing the material to expand into the new larger volume. The stresses normal to the wall in this case are then given by a Rankine active earth pressure, and result in Eq. (1) describing the

\* Corresponding author. Tel.: +1-3523039123; fax: +1-3528461196.  
E-mail address: kjohanson@erc.ufl.edu (K. Johanson).

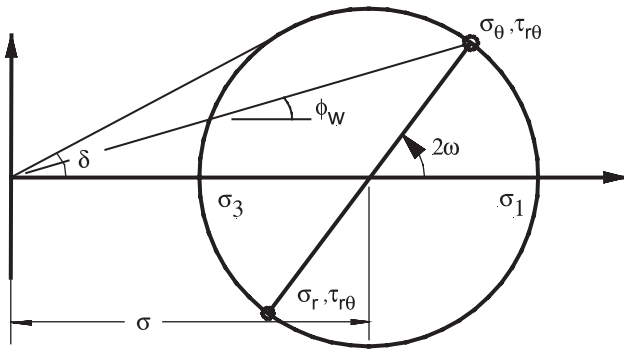


Fig. 1. Schematic of effective yield locus showing relationship between stresses.

ratio of normal wall stress to local vertical stress for a cohesionless material.

$$\frac{\sigma_3}{\sigma_1} = \frac{\sigma_w}{\sigma_v} = \frac{1 - \sin(\delta)}{1 + \sin(\delta)} \quad (1)$$

This produces stress ratios smaller than one. This same stress ratio exists in diverging bins and hoppers as material flows through them. Here the bin wall is stationary and the material moves away from the wall during flow. If the bin wall converges, then the stress ratio is given by Eq. (2) and results in stress ratios larger than 1.

$$\frac{\sigma_1}{\sigma_3} = \frac{\sigma_w}{\sigma_v} = \frac{1 + \sin(\delta)}{1 - \sin(\delta)} \quad (2)$$

In either case, the effective yield locus provides the boundary of all stress states that result in steady plastic flow. Plastic flow can exist in diverging or converging channels. The only difference between the two conditions is the direction of major principal stress. Converging geometries produce conditions where major principal stresses are directed predominately towards the bin wall. Diverging geometries yield conditions where minor principal stresses are directed towards the bin wall. Principal stresses are never completely normal to the wall since friction occurs along bin walls and principal stress conditions do not have shear stress acting on the principal plane. Instead, the direction of principal stress ( $\omega$ ) at the wall is computed from the intersection of the wall yield locus and the consolidation Mohr stress circle (Fig. 1). This relationship is given by Eq. (3).

$$\omega = \frac{1}{2} \left( \phi_w + \frac{\sin(\phi_w)}{\sin(\delta)} \right) \quad (3)$$

Stress normal to the wall is then given by Eq. (4) which relates the major principal stress at the wall to the effective

angle of internal friction ( $\delta$ ) and major stress direction angle ( $\omega$ ).

$$\sigma_w = \sigma_1 \left( \frac{1 \pm \sin(\delta) \cos(2\omega)}{1 + \sin(\delta)} \right) \quad (4)$$

The negative sign applies to diverging hoppers while the plus sign applies to converging geometries. This wall stress value is always less than the major principal stress at the wall for converging geometries, and always greater than the minor principal stress for diverging geometries implying that  $K$ -values in hoppers are bounded by the Rankine active and passive states given in Eqs. (1) and (2). In addition,  $K$ -values for bins and hoppers are defined as the ratio of the stress normal to the wall ( $\sigma_w$ ) to average vertical stress ( $\sigma_v$ ) across the channel as shown in Eq. (5).

$$K = \frac{\sigma_w}{\left( \frac{\int \sigma_y(A) dA}{A} \right)} = \frac{\sigma_w}{\sigma_v} \quad (5)$$

There is significant variation in vertical stress across converging flow channels. Vertical stress at the hopper centerline equals the minor principal stress while vertical stress at the hopper wall is lower than this centerline stress.

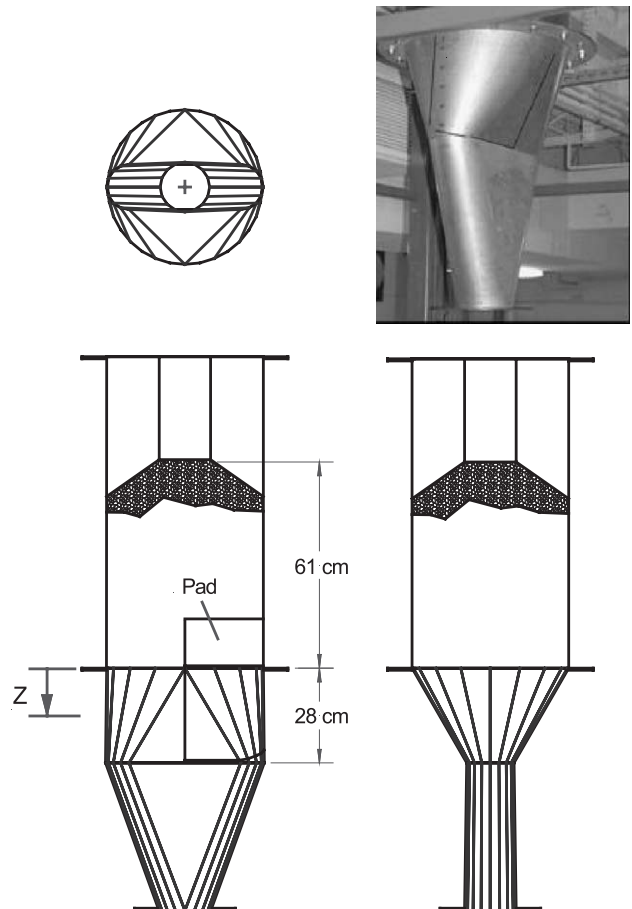


Fig. 2. Schematic of the Diamondback Hopper™ showing position of pad.

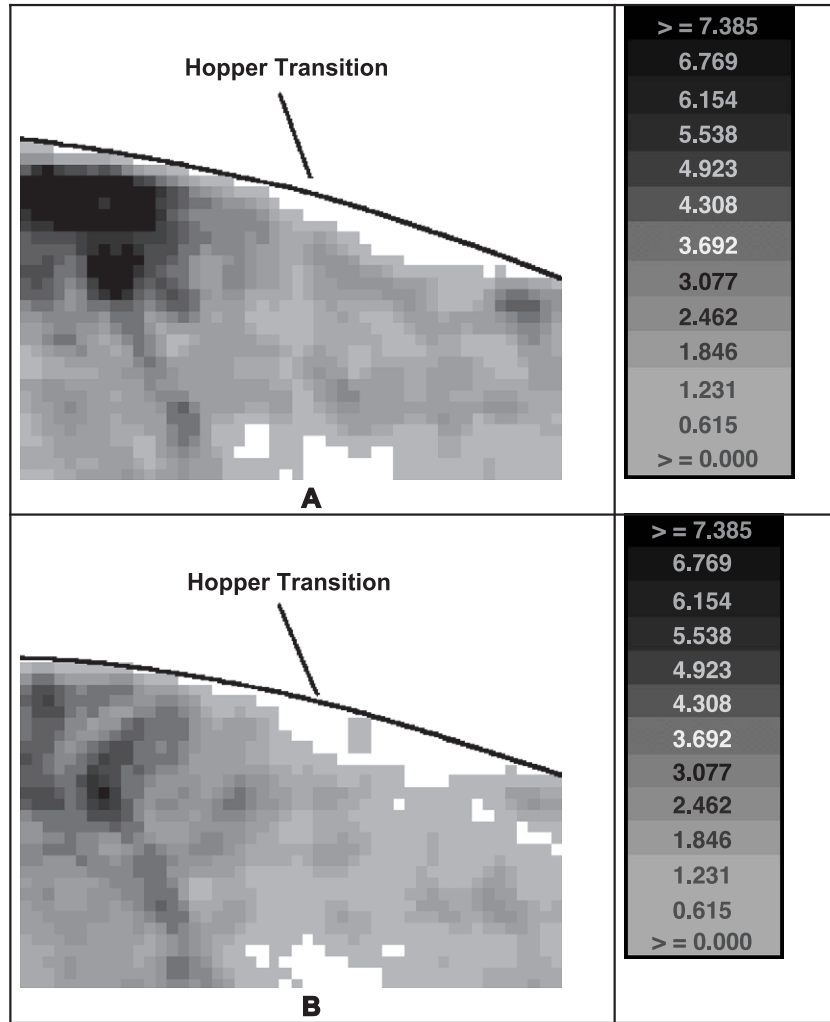


Fig. 3. Initial (A) and flow load (B) profile on TekScan™ pads showing stress concentration at the top of the triangular plate in the hopper. Left most loads are along the center of the triangular plate as shown in Fig. 2.

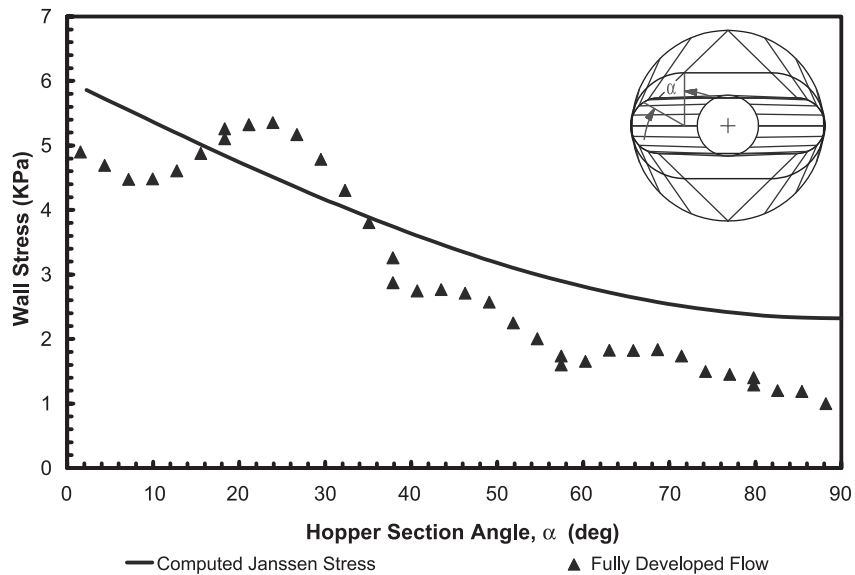


Fig. 4. Flow wall stresses at an axial position  $Z=3.8$  cm below the hopper transition.

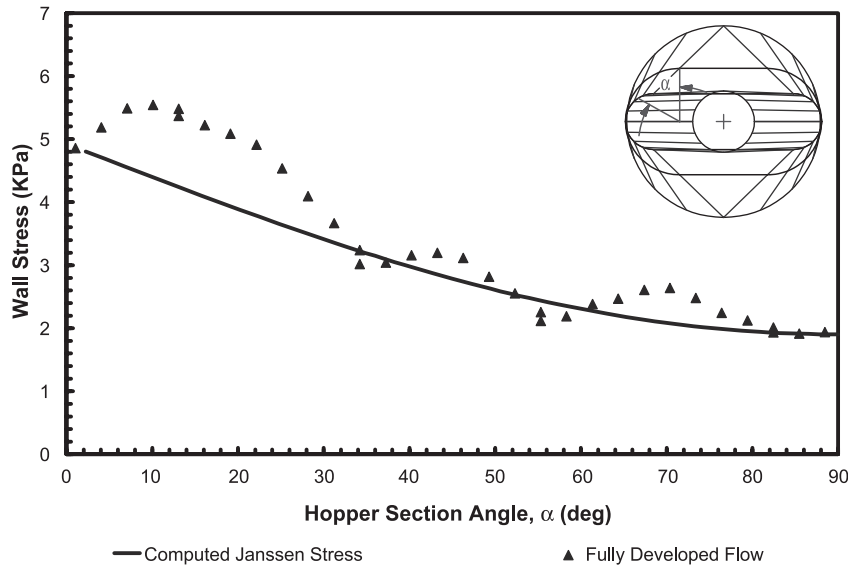


Fig. 5. Flow wall stresses at an axial position  $Z=6.3$  cm below the hopper transition.

As a result, the average vertical stress is always lower than the minor principal stress at the centerline. The wall stress is also considerably lower than the normal stress in the radial direction at the hopper centerline. In fact, the reduction of normal stress in the radial direction as the material approaches the wall is greater than the corresponding change in vertical stress.

The effects of variation in vertical stress and non-principal stress at the bin wall combine to produce typical converging  $K$ -values for conical channels that range between 1.6 and 2.6 for conical hopper angles close to the mass flow limit. Plane flow  $K$ -values are a little larger and range between 2.0 and 3.0 for typical plane flow hoppers.

Converging  $K$ -values cannot be greater than the passive Rankine stress ratio (Eq. (6)) and are typically much lower than this upper bound.

$$K_{\max} = \frac{1 + \sin(\delta)}{1 - \sin(\delta)} \tag{6}$$

Conversely,  $K$ -values in diverging hoppers cannot be any lower than the Rankine active stress ratio given in Eq. (7).

$$K_{\min} = \frac{1 - \sin(\delta)}{1 + \sin(\delta)} \tag{7}$$

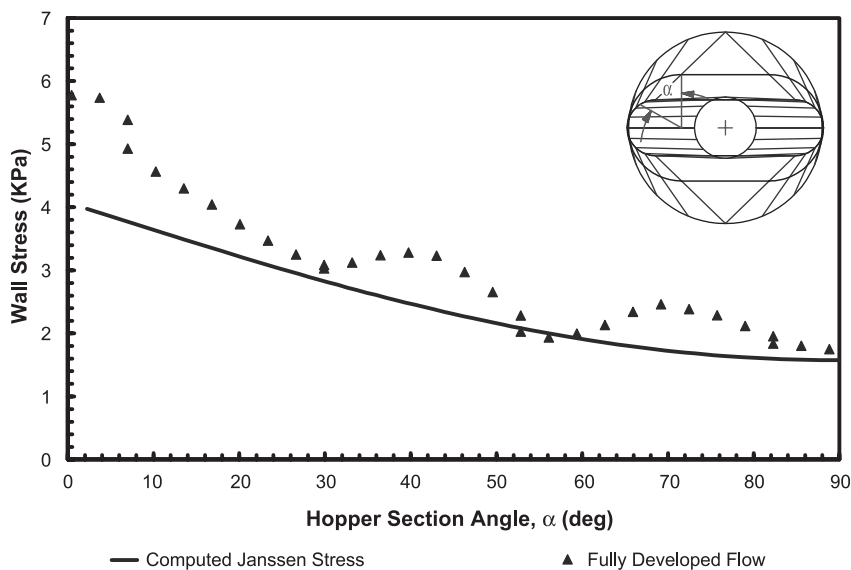


Fig. 6. Flow wall stresses at an axial position  $Z=8.9$  cm below the hopper transition.

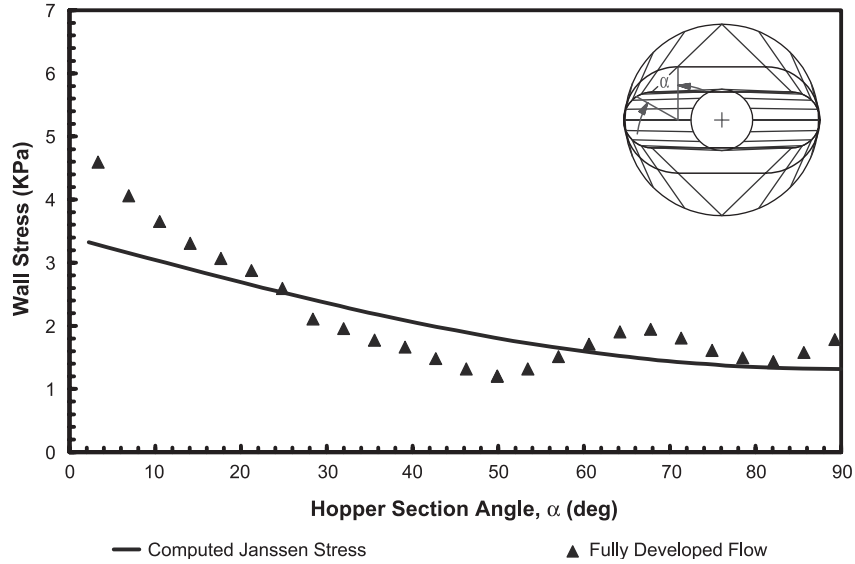


Fig. 7. Flow wall stresses at an axial position  $Z=11.4$  cm below the hopper transition.

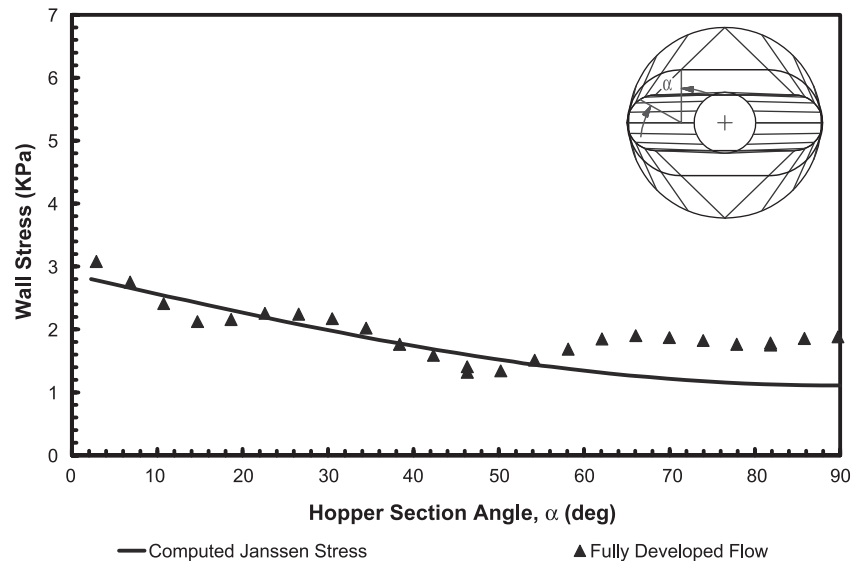


Fig. 8. Flow wall stresses at an axial position  $Z=14.0$  cm below the hopper transition.

The difficulty regarding the Diamondback Hopper™ is that the hopper converges in one direction and diverges in the other. It is reasonable to assume that local  $K$ -values may vary between these two limits given by Eqs. (6) and (7). In fact, a reasonable assumption is that local  $K$ -values depend on local hopper slope angle. This was validated by experimentation.

**3. Experimental results**

The Diamondback Hopper™ consists of a round-to-oval hopper with diverging end walls. This hopper section is positioned above an oval-to-round hopper that necks down to a circular outlet. Measuring the normal force along the

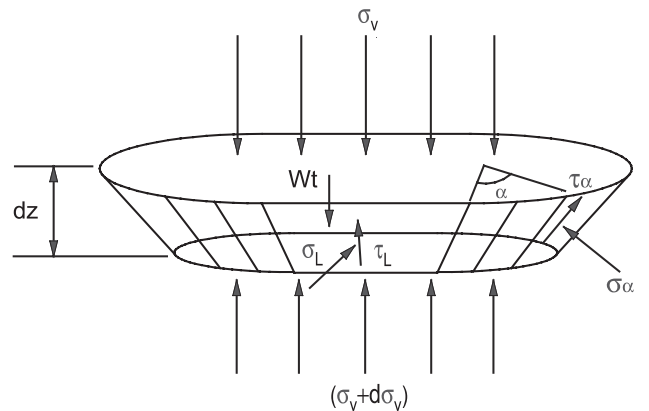


Fig. 9. Stresses acting on differential slice element.

Table 1  
Empirical  $K$ -values for Diamondback Hoppers™

Condition	$K_{1_{max}}$	$K_{1_{min}}$	$n$
Fully developed flow	2.2	0.85	1

surface of the hopper wall provides information that can be used to compute  $K$ -values for this unique hopper configuration. Pressure sensitive pads (from TekScan™) were used to measure the normal wall pressure. These pads consist of two plastic sheets with conductive pressure sensitive material printed in rows on one sheet of plastic and columns on the other sheet of plastic. When these sheets contact each other they form conductive junctions (sensors) where contact resistance varies with the normal stress applied. The effective area of each junction is 1 cm<sup>2</sup> and there are over 2000 independent normal stress measurements possible that can be recorded at cycle times up to eight per second. The voltage drops across these junctions were sequentially measured and scaled to give real engineering force units using the supplied data acquisition software. The TekScan™ pad was glued to the inside surface of the round-to-oval hopper with one edge of the pad along the center of the flat plate section (see Fig. 2).

Several pleats or folds were made in the upper portion of the pad to make it conform to the upper cylinder wall. A thin retaining ring was placed at the transition between the hopper and cylinder. This held the pad close to the hopper wall and helped maintain the pleats in the cylinder. Contact paper was placed on the hopper and cylinder surface to protect the pad and produce a consistent wall friction angle (of about 17°) in the bin. The pad lead was fed through the hopper wall well above the transition and connected to the data acquisition system. Spot calibration checks were per-

formed on groups of four load sensors (TekScan™ load measurement areas). This arrangement produced a load measurement system capable of measuring normal wall loads to within ± 10%.

The bin level was maintained by a choke fed standpipe located at the bin centerline and at an axial position about 60 cm above the hopper transition. The material used was fine 50 μm silica. During normal operation, the feed system maintains a repose angle at the bottom of the standpipe and produces a relatively constant level as material discharges from the hopper. Flow from the hopper was controlled by means of a belt feeder below the Diamondback Hopper™. There was a gate valve between the Diamondback Hopper™ and the belt. Initially, this gate was closed and the lower hopper was charged with a small quantity of material. The amount of material in the hopper initially was enough to fill only the lower oval-to-round section of the bin. The gate was then opened, allowing material to fill the void region between the gate and the belt. This was done to avoid surges onto the belt during the initial filling routine. The remaining hopper was then filled slowly, using the existing conveying system, until the Diamondback test hopper and a surge bin above this test hopper were filled. Material level was maintained in the surge hopper by recycling any material leaving the belt into the surge hopper feeding the Diamondback Hopper™ bin. Once the bin was full, material was allowed to stand at rest for about 10 min as material deaerated. The speed of the belt was preset and flow was initiated. The wall load data acquisition system recorded changes in wall stress as flow was initiated. Fig. 3 shows the wall loads measured on the TekScan™ pads just after initial fill (A) and after steady flow was achieved (B). The loads near the transition were large and similar in both cases. This large stress may be due to activation of the

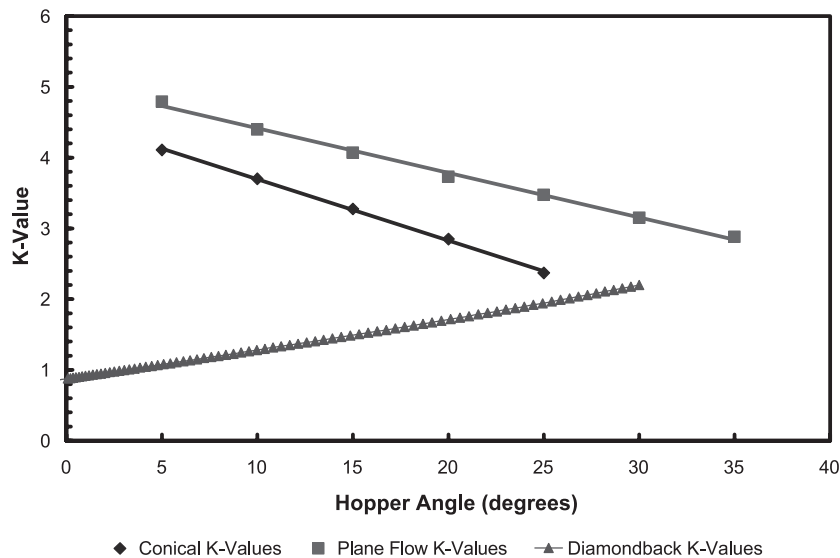


Fig. 10. Jenike  $K$ -values for conical and plane flow hopper geometries for an effective internal friction angle ( $\delta$ ) of 43° and a wall friction angle ( $\phi_w$ ) of 17°.

passive stress state caused by material settlement providing enough deformation to activate the wall friction and generate flow load conditions.

The initial stress condition shows a large peak pressure concentrating at the top point of the triangular flat plate in the hopper. This peak is focused at the tip of the plate. During flow these loads decrease and delocalize producing the highest peak stress measurements along the edge of the plate. Figs. 4–8 show the experimentally measured stresses around the hopper perimeter at constant axial depths. These stresses generally decrease around the perimeter and are smaller at greater material depths. Decreases in axial stress levels are typical in converging hoppers.  $K$ -values greater than one produce large frictional forces along hopper walls which partially supports the material in the hopper producing a decreasing axial stress. However, the decreasing stress values around the hopper periphery are caused by the unique Diamondback Hopper™ geometry.

#### 4. Janssen or slice model analysis

A force balance can be done on a small differential slice of material in the Diamondback Hopper™ as shown in Fig. 9. The forces acting on the material slice element are due to the bulk material slice weight, wall frictional forces on the flat plate section and the round end walls, vertical stresses, and normal stress conditions at the bin wall. The definitions of  $K$ -value and the Coulombic friction condition are used to relate the vertical pressure acting on the material to the stresses normal and tangent to the bin wall (see Eqs. (8)–

(11). The resulting differential equation is found in Eq. (12). The cross-sectional area ( $A$ ) and hopper dimensions ( $L$ ) and ( $D$ ) are functions of the axial coordinate as indicated in Eqs. (13)–(16).

$$\sigma_L = K_L \sigma_v \quad (8)$$

$$\tau_L = K_L \sigma_v \tan(\phi_w) \quad (9)$$

$$\sigma_\alpha = K_c(\alpha) \sigma_v \quad (10)$$

$$\tau_\alpha = K_c(\alpha) \sigma_v \tan(\phi_w) \quad (11)$$

$$\frac{d\sigma_v}{dz} = \gamma g - \left[ \frac{1}{A} \frac{dA}{dz} + \frac{2K_L(L-D)}{A} (\tan(\phi_w) + \tan(\theta_D)) + \frac{4D}{A} \int_0^{\pi/2} K_c(\alpha) (\tan(\phi_w) + \tan(\theta(\alpha))) \right] \sigma_v \quad (12)$$

$$A = \frac{\pi}{4} D^2 + (L - D)D \quad (13)$$

$$\frac{dA}{dz} = -2 \left[ \left( \frac{\pi}{2} - 2 \right) D + L \right] \tan(\theta_D) - 2D \tan(\theta_L) \quad (14)$$

$$L = L_T - 2z \tan(\theta_L) \quad (15)$$

$$D = D_T - 2z \tan(\theta_D) \quad (16)$$

The hopper wall slope angle changes around the perimeter. The slope angle along the flat plate section equals the hopper angle ( $\theta_D$ ), while the slope angle along the hopper end wall equals the hopper angle ( $\theta_L$ ). Variation in hopper

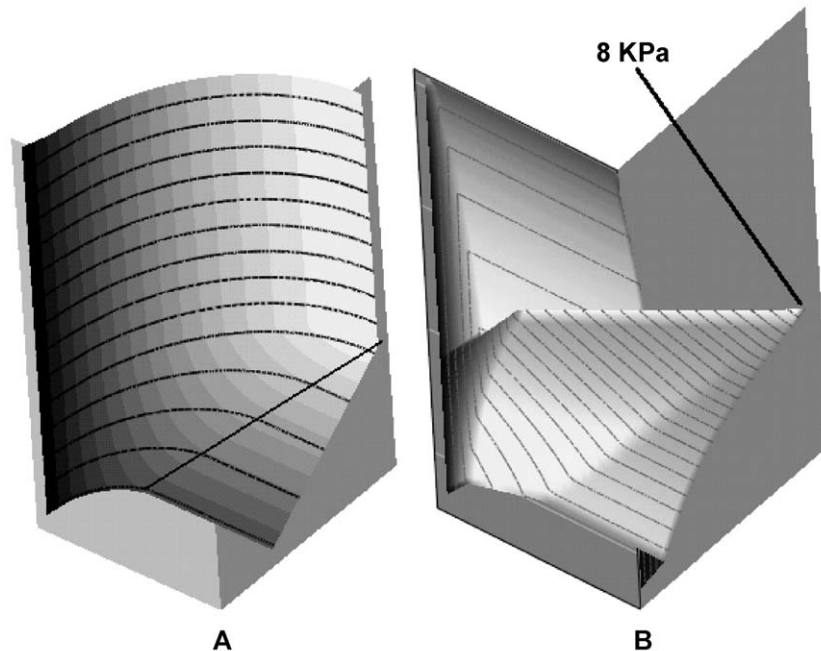


Fig. 11. 3D-view of wall stresses for flow loads in upper 1/4 hopper section. Loads show significant stress concentration at top of flat plate.

angle around the perimeter is given by Eq. (17) where  $(\alpha)$  is the hopper section angle as defined in Fig. 9.

$$\theta(\alpha) = \text{atan}[(1 - \sin(\alpha))\tan(\theta_D) + \sin(\alpha)\tan(\theta_L)] \quad (17)$$

The last relationship required to solve this differential equation is a description of how the  $K$ -value changes around the hopper perimeter. The Tekscan™ experiments indicated that wall stresses appeared to vary from a maximum value along the converging flat plate section of the hopper to a minimum value along the hopper end wall. The loads were then normalized by dividing the magnitude of the local wall stress by the magnitude of the maximum observed wall stresses at the same hopper elevation. This normalized stress data equals the ratio of the local  $K$ -value to the maximum  $K$ -value at any elevation. It is a function of position around the hopper perimeter (see Eq. (18)).

$$\frac{K_e(\alpha)}{K1_{\max}} = f(\alpha) \quad (18)$$

Several curve fit functions  $f(\alpha)$  were used in an attempt to empirically fit the experimental load profile. A general least squares analysis was used to determine the best fit for the load data suggesting that load profiles around the perimeter could be reasonably well represented by a  $\sin(\alpha)^n$  function. Eq. (19) shows the resulting empirical equation describing the  $K$ -value as a function of hopper section angle  $(\alpha)$ .

$$K_e(\alpha) = (K1_{\min} - K1_{\max})(\sin(\alpha)^n) + K1_{\max} \quad (19)$$

Eq. (12) was combined with results from Eq. (19) and integrated numerically to give the computed wall stress profile. Values of parameters  $K1_{\min}$ ,  $K1_{\max}$ , and  $n$  were chosen to minimize the deviation between the observed wall stress profiles and the calculated wall stresses over the entire axial hopper depth. Reasonable fits were obtained for flow wall stress profiles by using the parameters shown in Table 1.

Figs. 4–8 compare calculated Janssen stress profiles for fully developed flow conditions with experimental data. There is reasonable agreement between the Janssen model and observations in predicting the general trend for local wall stresses. However, the experimental wall stresses fluctuated spatially, causing some deviation from the model. For flow conditions, the maximum  $K$ -value is 2.2 while the minimum  $K$ -value is 0.85. Plane flow  $K$ -values for wedge shaped hoppers can be computed using Jenike load charts [2]. These charts yield a  $K$ -value of 3.15 for a 30° wedge shaped hopper with material having a 17° wall friction angle and an effective friction angle of 43° (see Fig. 10).

This suggests that maximum  $K$ -values in Diamondback Hoppers™ are lower than plane flow hoppers and are closer to the expected  $K$ -values in mass flow conical hoppers. However, the  $K$ -value decreases around the bin perimeter, causing the average  $K$ -value in Diamondback Hoppers™ to be lower than this maximum value. This will cause vertical stresses in Diamondback Hoppers™ to be larger than the

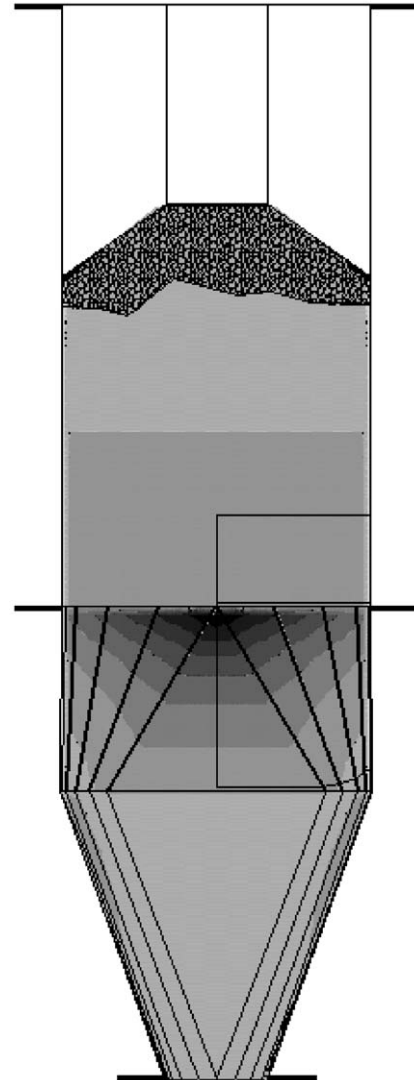


Fig. 12. Projected contour plot of wall stresses for flow loads in upper hopper section. Loads show significant stress concentration (black) at top of flat plate and lower stress at hopper end walls (light gray).

corresponding stresses in conical hoppers. Fig. 11 shows a qualitative 3D-view of expected wall stresses in the upper Diamondback Hopper™. These stresses apply to one quarter of the hopper as shown in Fig. 11A. The stresses normal to the hopper wall are shown in Fig. 11B. Fig. 12 shows a projected contour plot of calculated wall stress for the fully developed flow condition. Both these figures reveal a large peak stress at the top of the triangular flat plate in Diamondback Hoppers™. They also show a significant decrease in wall stresses around the hopper perimeter.

## 5. Conclusions

The Diamondback Hopper™ has a unique variation in  $K$ -values depending on the position in the hopper. These

$K$ -values indicate a rotation of principal axes in the hopper around the hopper perimeter. The likely reason for this rotation of principal direction is the converging–diverging nature of the hopper. This change in major principal direction produces the net effect of average Diamondback Hopper™  $K$ -values lower than either conical or plane flow hoppers. The Janssen slice model can provide a first approximation to the loads in Diamondback Hoppers™. However, there is significant variation from the simple slice model approach used here. More complex constitutive models will be required to increase the agreement between experimental and theoretical approaches. Pressure sensitive pads are a useful tool in examining spatial variation in hopper wall loads.

## 6. Nomenclature

$A$	Hopper cross-sectional area.	$dz$	Depth of differential slice element.
$D$	Diameter of flow channel perpendicular to oval hopper axis as a function of axial position.	$\alpha$	Hopper section angle.
$D_T$	Diameter of flow channel perpendicular to oval hopper axis at top of bin.	$\gamma$	Powder bulk density.
$K$	Janssen $k$ -value ratio of stress normal to the wall to the vertical stress in the axial direction.	$\theta$	Local hopper angle.
$K_{\max}$	Largest Janssen $k$ -value ratio for converging hopper geometries.	$\theta_D$	Hopper angle perpendicular to oval axis of hopper.
$K_{\min}$	Smallest Janssen $k$ -value ratio for diverging hopper geometries.	$\theta_L$	Hopper angle parallel to oval axis of hopper.
$K_L$	Janssen $k$ -value ratio on flat plate section	$\delta$	Effective Internal friction angle.
$K_e$	Janssen $k$ -value ratio around hopper end wall.	$\phi_w$	Wall friction angle.
$K1_{\max}$	Largest local Janssen $k$ -value ratio in hopper at flat plate surface.	$\sigma_r$	Normal stress on the plane perpendicular to the radial direction in a cylindrical coordinate system.
$K1_{\min}$	Smallest local Janssen $k$ -value ratio in hopper at end wall location.	$\sigma_\theta$	Normal stress on the plane perpendicular to the $\theta$ -direction in a cylindrical coordinate system.
$n$	Curve fit parameter for local $k$ -value function.	$\sigma$	Mean stress.
$L$	Length of oval axis in hopper as a function of axial position.	$\sigma_L$	Normal stress on flat plate surface.
$L_T$	Length of oval axis in hopper at top of bin.	$\sigma_\alpha$	Normal stress around end wall of hopper.
$Wt$	Weight of material in differential slice element.	$\tau_L$	Shear stress on flat plate surface.
		$\tau_\alpha$	Shear stress around end wall of hopper.
		$\sigma_3$	Minor principal stress.
		$\sigma_v$	Average vertical stress for Janssen analysis.
		$\tau_{r\theta}$	Shear stress on the plane perpendicular to the radial direction acting in the $\theta$ -direction in a cylindrical coordinate system.
		$\omega$	Angle between the major principal stress and the $\theta$ -coordinate direction.

## Acknowledgements

The author would also like to acknowledge the financial support of the Engineering Research Center (PERC) for Particle Science and Technology at the University of Florida, the National Science Foundation NSF Grant #EEC-94-02989, and the Industrial Partners of the PERC.

## References

- [1] H.A. Janssen, Versuche über getreidedruck in silozellen, Z. Ver. Dtsch. Ing. 39 (1895) 1045–1049.
- [2] A.W. Jenike, Gravity flow of bulk solids, Bulletin, vol. 108, Utah Engineering Station, 1961.